A NEW Fe-He INTERATOMIC POTENTIAL BASED ON *Ab Initio* CALCULATIONS IN α-Fe –
F. Gao, H. L. Heinisch, R. J. Kurtz (Pacific Northwest National Laboratory)

OBJECTIVE

The objective of this research is to develop multiscale models describing the transport and fate of He and its effect on microstructural evolution in ferritic steels irradiated in a fusion environment. Previous molecular dynamics investigations of He bubble formation and He-vacancy clustering were performed using a Fe-He pair potential developed by Wilson and Johnson, but the relative stability of octahedral and tetrahedral interstitial He atoms is inconsistent with that determined by *ab initio* methods and, more importantly, the binding energies of He atoms to He-vacancy and interstitial He clusters are much higher than those determined from *ab initio* calculations. Consequently, a new Fe-He potential has been developed to better reproduce the *ab initio* results.

SUMMARY

A new interatomic potential for the Fe-He interaction has been developed by fitting to results obtained from *ab initio* calculations. Based on electronic hybridization between Fe d-electrons and He s-electrons, an s-band model, along with a repulsive pair potential**,** has been proposed to describe the Fe-He interaction. The atomic configurations and formation energies of single He defects and small interstitial He clusters are considered in the fitting process. The binding properties and relative stabilities of the He-vacancy and interstitial He clusters are studied, and the results are compared with available *ab initio* calculations as well as with those obtained from previous Fe-He potentials. The present Fe-He potential overcomes the disadvantages that appear in previous Fe-He potentials, and it will be applied to simulate the interactions of He with Fe in various microstructural features in large-scale molecular dynamics simulations.

PROGRESS AND STATUS

Introduction

Understanding the interactions of a helium impurity with metal atoms is of fundamental importance within a fusion reactor environment, where the first wall will be exposed to a high flux of helium generated under irradiation by (n,α) transmutation reactions [1]. The accumulation of helium atoms in materials can result in the formation of helium bubbles, which can lead to void swelling and produces high temperature intergranular embrittlement, surface roughening and blistering [2]. These phenomena can significantly degrade the mechanical properties of materials. A detailed study of how He interacts with various microstructures is needed to develop a multi-scale model for prediction of long-time material behavior in the high helium environment of a fusion reactor. At the atomic-level molecular statics, molecular dynamics and the dimer method of potential surface mapping have been used to understand helium behavior in alpha-iron, such as the fate of He atoms in the vicinity of dislocations [3], the migration of He interstitials and He-vacancy clusters [4], and He effects on the primary damage state and subsequent defect evolution [5,6]. However, the results obtained from these simulations are found to depend on the empirical potentials used in the Fe-He system.

In early molecular statics and dynamics simulations most studies of He behavior in Fe employed the repulsive Fe-He potential of Johnson and Wilson [7], which predicts the most stable He interstitial position to be in the octahedral configuration, in contrast to the recent *ab initio* calculations [8] that demonstrated that the tetrahedral interstitial position is the most stable configuration. Furthermore, when using the Johnson and Wilson potential the binding energies of a He atom to both He_xV and He_x clusters (x=1 to 10) are much higher than those determined from *ab initio* calculations. In recent years new empirical Fe-He potentials have been developed. Seletskaia et al. [9] argued that, along with a repulsive pair-potential form, a three-body interaction term is needed to produce a more stable tetrahedral He interstitial relative to the octahedral configuration. Detailed calculations with this potential indicate that a singularity exists in

the force when the angle between a He atom and an Fe atom is 0° or 180°, which may cause the octahedral He interstitial to be unstable. However, the binding energies of He clusters calculated using this new potential are in good agreement with those obtained from *ab initio* calculations. On the other hand, Juslin and Nordlund (JN) have demonstrated that an Fe-He pair potential is sufficient to describe the relative stabilities of single He interstitials [10], since He is a noble gas atom. However, the binding energies of small He clusters calculated using the JN potential are too small relative to the *ab initio* calculations, and also, the potential has a force discontinuity at a distance of 0.12 nm.

We report here on the development of a new Fe-He potential that is based on an "s-band model." Using the Ackland et al. potential [11] for the Fe-Fe interactions, the atomic configurations and formation energies of single He defects and small interstitial He clusters are considered in the fitting process. The binding properties and relative stabilities of the He-vacancy and interstitial He clusters are studied, and the results are compared with available *ab initio* calculations, as well as with those obtained from previous Fe-He potentials.

Fitting Interatomic Potential

Ab initio calculations

It may be difficult to directly determine from experiments the detailed configurations and relative stabilities of He atoms in materials at the scale needed for understanding He behavior. Thus, obtaining this information for our purposes largely depends on *ab initio* calculations in the framework of density functional theory (DFT). The atomic configurations, formation energies and binding properties of He defects and He-V clusters in metals have been studied by different groups [9,12,13], using either VASP or SIESTA codes. In general, all the calculations demonstrate that the He tetrahedral is the most stable interstitial in Fe. The formation energies of He defects and small clusters are listed in Table 1. In the fitting process, the formation energy of a He_nV_m cluster is defined as following:

$$E_f(He_nV_m) = E_{tot}(He_nV_m) - [nE^c_{He} + (N-m)E^c_{Fe}], \quad (1)$$

where N is the total number of Fe atoms in a perfect crystal, and E_{He}^c and E_{Fe}^c are the cohesive energies of a perfect fcc He crystal and a perfect bcc Fe crystal, respectively. The binding energy of a He to the He_nV_m cluster can then be calculated by

$$E_b(He) = E_f(He) + E_f(He_nV_m) - E_f(He_{n+1}V_m), \quad (2)$$

where $E_f(He)$ is the formation energy of a single He interstitial in Fe.

Table 1. Formation energies of He defects in Fe calculated from *ab initio* methods, along with those obtained by different potentials for comparison. All the values are in eV.

Defect	VASP[a](ORNL)	SIESTA[b] (Fu)	ORNL[a](pot)	Juslin[c] (pot)	Present
He sub	3.84 – 4.08	4.22	3.75	4.10	3.71
He tetra	4.37	4.39	4.26	4.39	4.42
He oct	4.60	4.58	4.57	4.51	4.47
He-He-V	6.61		6.46		6.79
He-He-He-V	9.28		9.37		9.88
He-He	8.79		8.24		8.54

[a]Reference [9]
[b]Reference [12]
[c]Reference [10]

More recently, the binding properties of He defects and host atoms have been characterized using the total electronic density of states and charge densities of Fe atoms due to a He interstitial [13]. Fig. 1 shows the changes of the charge densities produced by the He octahedral and tetrahedral defects in Fe. It is of interest to find that the He interstitial and its nearest neighbor Fe atoms are all polarized due to the interactions between them with and without spin polarization, which arises from electronic hybridization between Fe d- and He s-electrons. It should be noted that the bonding interaction due to electronic hybridization is weak since He has a closed-shell electronic structure. However, this demonstrates that the electron density is dependent on the local environment in a Fe-He system.

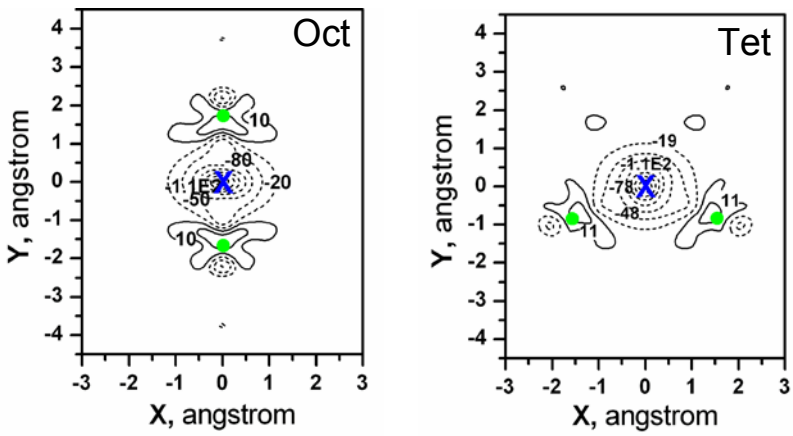

Fig 1. Changes in the charge densities of Fe atoms due to the presence of a He interstitial in octahedral and tetrahedral locations, where the structures are fully relaxed. The lines represent contours of equivalent charge density (*10^3) with the same separation of 0.03*e*/Å^3, where the solid lines indicate an increase in charge density and dashed lines represent charge depletion. The cross indicates the position of He and filled green circles specify the positions of its nearest-neighbor Fe atoms.

Fitting Methodology

The pair interaction and the many-body functional for Fe were taken from the work of Ackland et al. [10], while the pair potential developed by Aziz et al. [14] that describes He properties in vacuum was used for the He-He interaction in Fe. Similar to the many-body potential formalism, the potential for the Fe-He interaction consists of a pair potential and an embedding function, and then the total energy of an Fe-He system can be written as

$$U = \sum_{i=1}^{N-1} \sum_{j=i+1}^{N} V(r_{ij}) + \sum_i F_d(\rho_d^i) + \sum_i F_s(\rho_s^i), \tag{3}$$

where the first term represents a purely repulsive potential and the second and third terms are the many-body terms that provide the contribution due to electron density, as discussed before.

$$V(r) = \sum_{k=1}^{8} a_k (r_k - r)^3 H(r_k - r), \tag{4}$$

$$F_k(\rho_k) = b_1^k \sqrt{\rho_k} + b_2^k \rho_k^2 + b_3^k \rho_k^4, \tag{5}$$

where k indicates the s- or d-band model. These functions are the same as those for the Fe-Fe interaction, and are relatively easy to compute. For the mixed-pair electron density, we have employed the 1s-type and 4d-type Slater functions for He and Fe [15], respectively, but without considering the directional bonding of 4d electrons in Fe:

$$\chi^{1s} = N_{1s}\, exp(-\xi r)\,, \tag{6}$$

$$\chi^{4d} = N_{1d} r^3\, exp(-\xi r)\,. \tag{7}$$

The electron density for one Fe-He pair is the product of eqs. (6) and (7);

$$\phi_s^{FeHe} = N_s r^3\, exp(-2\xi_s r)\,, \tag{8}$$

where ξ_s is an average ξ from single ξ approximations of the 4d and 1s Hartree-Fock Fe and He orbitals, with a natural cutoff distance at 4.1 Å. N_s is equal to N_{1s} times N_{1d}, and it is chosen to be 20.0, so that the s-electron density at the first nearest-neighbor distance is equal to 0.01%. This demonstrates that the contribution to the total energy from s-electrons is very small, which is consistent with *ab initio* observations. The total electron density of an atom calculated from s-band model is given by

$$\rho_s = \sum \phi_s^{FeHe}(r) \tag{9}$$

The potential parameters are fitted using a least-squares fitting procedure with the objective function, U, defined as

$$U = \sum w_i [\, f_i(\lambda) - F_i \,]^2\,, \tag{10}$$

which determines the goodness of fit of each individual set. The calculated properties f_i depend on N parameters λ. The smaller the value of U, the closer is $f_i(\lambda)$ to the reference values F_i. The weight of each data item i in the fit, denoted w_i, determines how well the final fit will reproduce each property. Also, the atomic configurations of He defects and clusters are spontaneously relaxed using classical molecular static relaxation in a 432-atom cell during the fitting. I n the present fitting, the defect formation energies of relaxed substitutional, octahedral, and tetrahedral He interstitials and some small He-V and He-He clusters are used, and these values calculated using SIESTA and VASP are listed in Table 1.

Results

Interatomic Potential

The parameters of the pair potential and the many-body interaction are given in Table 2, while the pair potential and density function of Fe-He interaction are presented in Figs. 2 (a) and (b), respectively, along with those of Fe-Fe and He-He interactions for comparison. It can be seen that the contribution of s-electrons to many-body interaction is much smaller than that from d-electrons of Fe atoms.

Table 2. Parameters for pair potential and many-body interaction given by Eqs. (4) and (5).

Pair Potential		**s-band Model**
a_k(eV/Å^3)	**r_k(Å)**	**b_k^s (eV)**
a_1= 35.094090416476	r_1=1.35	b_1= 0.205594333601
a_2= -45.327101078621	r_2=1.50	b_2= 0.726210815237
a_3= 552.620374840293	r_3=1.65	b_3= 3.390462179478
a_4= 162.211114487242	r_4=1.80	N_s= 20.0 (Å^{-3})
a_5= -1.705295512930	r_5=2.00	ξ_s= 2.8936295071479 Å^{-1}
a_6= 0.105401602643	r_6=2.50	r_{cut}=4.1 Å
a_7= 0.072769270707	r_7=3.50	
a_8= 0.037744606924	r_8=3.90	

Formation and Binding Properties of He Defects

The results of the fitting procedure for single He defects and small He clusters are given in Table 1, together with those calculated by other empirical potentials for comparison. In general, the potential reproduces the formation energies of He defects reasonably well, and the tetrahedral He interstitial is the most stable configuration in all the iron matrices. The most stable configuration of a He_2-V cluster is found to be a <100> dumbbell, with a formation energy of 6.79 eV and a separation distance of 1.6 Å, in excellent agreement with the values calculated by *ab initio* methods. The new potential somewhat overestimates the formation energy of a He_3V cluster, but the binding energy of a He di-interstitial is determined to be 0.31 eV, in good agreement with 0.28 eV calculated by the three-body Fe-He potential, and slightly smaller than the value of 0.48 eV obtained using SIESTA.

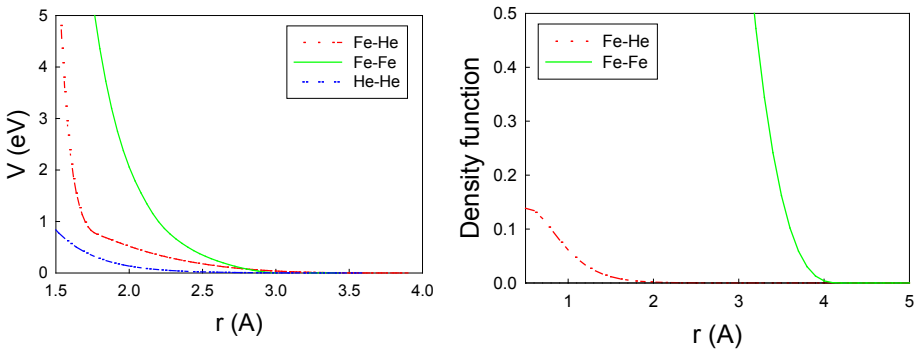

Fig. 2. (a) The repulsive pair potentials for Fe-He, Fe-Fe [11] and He-He [14] interactions, and (b) the density functions for Fe-He and Fe-Fe interactions.

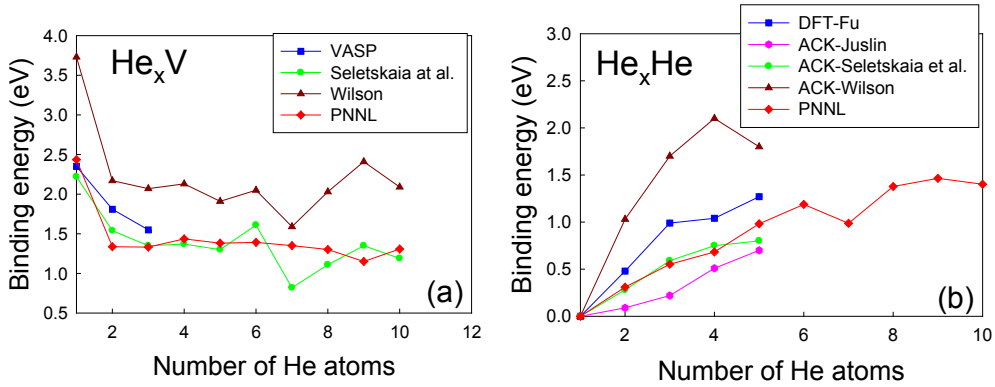

Fig. 3. (a) Binding energy of an additional He atom to a He-V cluster, and (b) binding energy of an additional He atom to a He-He cluster.

The newly developed Fe-He potential has been employed to study the properties of He-V and He-He clusters, and their binding energies as a function of cluster size when a He atom is added to He-V or He-He cluster. A cubic computational cell of $10a_0$x$10a_0$x$10a_0$ units (a_0 – bcc iron lattice constant) was used, and periodic boundary conditions were applied in all directions. The atomic configurations were relaxed using a molecular statics approach at 0 K, with a constant volume condition. The results for a He atom binding to a He-V cluster and a He-He cluster are presented in Figs. 3 (a) and (b), respectively. The binding energies calculated from first principles, and the previous Fe-He potentials are imposed for comparison. The binding energies calculated with the current Fe-He potential are slightly smaller than those obtained from first principles, but they are generally in good agreement with those calculated from Seletskaia's Fe-He potential. Wilson's potential systematically overestimates the binding of a He atom to both the He-V cluster and the He-He cluster.

The binding energy of an additional He atom to the He-V cluster initially decreases and then remains almost a constant value of about 1.3 eV. In the calculations by Seleskaia et al., there exists a local maximum when a total of six He atoms are involved in a He-V cluster that forms a He compact octahedron with a vacancy at the center, whereas a sudden decrease in the binding energy occurs for a He-V cluster with seven He atoms. In the latter case, the local dilatations produced by the cluster are strong enough to begin displacing iron atoms at the periphery of the cluster, which is responsible for this decrease. In the present study, the dilatations around a He-V cluster have been observed to occur when a cluster contains He atoms larger than four, and they increase with increasing cluster size. However, a compact He octahedron is also observed in the present simulations for a cluster containing six He atoms, which is in consistent with the previous investigations.

The binding energy of an additional He atom to a He cluster generally increases with increasing cluster size, as shown in Fig. 3(b), and it approaches a value of about 1.4 eV when the total number of He atoms is larger than eight. The binding energies calculated with the new potential agree with *ab initio* calculations within 0.25 eV, and they are in excellent agreement with those for small He clusters calculated by Seletskaia at al. It should be noted that the binding energies of small He clusters determined using Juslin and Nordlund's Fe-He potential is very small (~0.1 eV), which suggests that the small He clusters can easily dissociate, even at low temperatures. This may account for the significant differences between the results using the present potential and Juslin and Nordlund's potential. It has been observed that significant matrix distortions occur for large He clusters for the present simulations, leading to large displacements of the neighboring Fe atoms. This may suggest that interstitial Fe clusters can be directly generated through a so-called loop punching mechanism, which needs to be further investigated using molecular dynamics simulations.

CONCLUSIONS

Based on *ab initio* studies, we have proposed an s-band model to develop a new interatomic potential for the Fe-He interaction using a relaxation-fitting approach, using a least-squares fitting technique. The atomic configurations and formation energies of single He defects and small interstitial He clusters are considered in the fitting process. Calculations using the new potential demonstrate that both tetrahedral and octahedral interstitials are stable, but tetrahedral He forms the most stable configuration. The binding properties and relative stabilities of He-vacancy and interstitial He clusters are studied, and compared with available *ab initio* calculations as well as with results obtained from previous Fe-He potentials. The results are in reasonable agreement with both the *ab initio* and previous potential calculations. The present Fe-He potential represents an important improvement over currently available potentials because it overcomes the disadvantages existing in previous Fe-He potentials, and it can be easily applied to study the interactions of He with Fe in various microstructural features in large-scale molecular dynamics simulations.

References

[1] S.J. Zinkle, Phys. Plas.12, 058101 (2005).
[2] Y. Katoh, M. Ando, and A. Kohyama, J. Nucl. Mater. 323, 251 (2003).
[3] H.L. Heinisch, F. Gao, R.J. Kurtz and E.A. Le, J. Nucl. Mater., in press.
[4] F. Gao, H.L. Heinisch and R.J. Kurtz, J. Nucl. Mater. 386-288, 390 (2009).
[5] L. Yang, X. T. Zu, H. Y. Xiao, F. Gao, H. L. Heinisch, R. J. Kurtz and K. Z. Liu, Appl. Phys. Lett. 88, 091915 (2006).
[6] G. Lucas and R. Schaeublin, J. Phys.: Condens. Mater. 20, 415206 (2008).
[7] W. D. Wilson and R. D. Johnson, Proceedings Interatomic Potentials and Simulation of Lattice Defects, Plenum, New York (1972) 375.
[8] T. Seletskaia, Y. Osetsky, R.E. Stoller, G.M. Stocks, Phys. Rev. Lett. 94, 046403 (2005).
[9] T. Seletskaia, Yu. N. Osetsky, R. E. Stoller, and G. M. Stocks, J. Nucl. Mater. 367-370, 355 (2007).
[10] N. Juslin and K. Nordlund, J. Nucl. Mater. 382, 143 (2009).

[11] G. J. Ackland, M. I. Mendelev, D. J. Srolovitz, S. Han and A. V. Barashev, J. Phys.: Condens. Mater. 16, 52629 (2004).
[12] C. C. Fu and F. Willaime, J. Nucl. Mater. 367-370, 244 (2007).
[13] X. T. Zu, L. Yang, F. Gao, S. M. Peng, H. L. Heinisch, X. G. Long and R. J. Kurtz, Phys. Rev. B80, 0541041 (2009).
[14] R. A. Aziz, A. R. Janzen and M. R. Moldover, Phys. Rev. Let. 74, 1586 (1995).
[15] E. Clementi and C. Rostti, Atomic data and nuclear data tables 14, 177 (1974).